Journal of Basic and Applied Engineering Research
p-ISSN: 2350-0077; e-ISSN: 2350-0255; Volume 2, Issue 20; October-December, 2015, pp. 1785-1789

http://www.krishisanskriti.org/Publication.html

Synthesis of ZnO/ZnS core/shell Nanostructures for its Possible Fabrication as Photoconductors

Sujata Deb[1], P.K. Kalita[2] and P. Datta[3]

[1,2,3]Gauhati University, Guwahati-781014, Assam, India
E-mail: [1]sujatabmk@gmail.com, [2]pkkalitagc@gmail.com, [3]pranayee.datta@gmail.com

Abstract—*ZnO-ZnS core-shell nanostructures according to three different core-shell volume metric ratios (1:1.5), (1:2.25) and (1:3) have been successfully synthesized* via *chemical bath deposition (CBD) technique using starch as capping agent. The morphology and structure of the product and the precursor are verified by x-ray diffraction (XRD) and high resolution transmission electron microscopy (HRTEM). The XRD of the core / shell film shows the presence of hexagonal wurtzite type ZnO nanostructure and the cubic phase of ZnS. The HRTEM results confirm that the as-prepared product is ZnO-ZnS core-shell nanostructures indicating that ZnS was formed on the surface of ZnO. The UV–vis absorption spectra of the ZnO-ZnS core-shell nanostructures exhibit a blue shift in the absorption edge due to the quantum confinement effect. The PL emission spectra of all the ZnO–ZnS core–shell nanostructures are compared with the ZnO nanostructures.. And it is inferred that with the increase in shell thickness, the PL intensity decreases whereas conductivity is found to increase, which indicates the separation of charge. Hence, the nanostructures are expected to be a suitable candidate for photoconductors and are a subject of further investigation.*

1. INTRODUCTION

Controlling materials within the dimension of a few nanometers to a micrometer has become a great field of research for materials scientists over the past few decades. Among the various study, core-shell nanostructures comprising of two important functional constituents of II-VI compounds that exhibit material-dependent properties have become the center of intensive research[1-2]. Such novel passivated ensembles are extensively more tunable than single-constituent materials, thus their study extends wide scope of applications. A wide range of core-shell nanostructures have been synthesized and studied by choosing the appropriate temperature, solvent, or coordinating ligands[3-4]. In recent times, ZnO-ZnS core-shell nanostructures have attracted pronounced attention because of their potential applications in nanoscale electronics, magnetism, catalysis, sensing devices, optics, and other novel devices [5]. Zinc oxide (ZnO) is an n-type semiconductor with a wide direct band gap of 3.37 eV at room temperature and has a large binding energy (60meV). It has gained a tremendous amount of theoretical and experimental interests due to its unique nanoscale range of technological applications including conductive layer in solar cells, UV emitter, transparent conducting electrodes of solar cells, flat panel displays, surface acoustic wave devices, and sensors [6-9]. On the other hand, zinc sulfide (ZnS) is a wide band gap semiconductor with band gap of 3.7eV at room temperature and has large exciton binding energies of 40 meV. It is a recognized luminescence material having noticeable applications in flat-panel displays, sensors, lasers and also has been applied in nonlinear optical devices.[10]. Besides, both the materials are abundant, extremely stable, and biologically friendly. Although, works have been reported on ZnO ZnS core/shell nanostructures[11], it is furthermore feasible to engineering new materials. Most of the works reported the enhancement of optical properties of these nanostructures materials. And, there are few reports on quasitype-II structure formation[12]. In type I core-shell nanostructures, the electron and holes tend to localize within the core, whereas, in type II structures, one carrier is localized in the shell while the other is localized in the core. [13]Surface passivation of ZnO by ZnS coating is found to suppress the photoluminescence of the core ZnO by reducing the recombination probability of the charge carriers but then again enhance the photocurrent, indicating spatial separation of electrons in the core and holes in the shell region. Thus, charge recombination is minimized to create photovoltaic effect. Wang *et al.* [12] synthesized a vertically aligned ZnO/ZnS core/shell nanowire array and investigated the photovoltaic effect. Dutta *et al.* [14] studied the effect of ZnS coating over ZnO core. Various construction routes including Chemical Vapor Deposition (CVD), chemical vapor decomposition, Pulse Laser Deposition (PLD) techniques, thermal sulfidation, etc. have been employed, but, chemical bath de-position (CBD) method is presently inviting considerable attention as it does not require sophisticated tools and is relatively inexpensive.

In this study, we report the synthesis of ZnO-ZnS core-shell nanostructures with three different core-shell volume metric ratios (1:1.5), (1:2.25) and (1:3) via CBD method at a temperature of around 100 °C using starch as a capping agent, to provide stable surface passivation. Investigation regarding the effect of the shell thickness on the optical and photoconductive properties of the nanostructures has been

studied. The results indicate that, with the increase in shell thickness, the PL intensity decreases whereas conductivity increases, which direct the separation of charge, thus ZnO-ZnS Core-Shell nanostructures may act more efficiently as photoconductors.

2. EXPERIMENTAL SECTION

Synthesis

Three samples of core/shell ZnO/ZnS with different volume metric ratios (1:1.5), (1:2.25) and (1:3) via chemical bath deposition method are prepared by using starch as capping agent. The ratio of the molar volumes of core ZnO to shell ZnS are 1:1.5, 1:2.25 and 1:3 for sample-I, sample –II and sample-III respectively. All the chemical reagents purchased for the experiment are of analytical grade (Merck) and are used without any alteration. The synthesis process consisted of two phases. The first phase (i) the development of core ZnO nanostructures and (ii) the formation of a ZnS shell to encapsulate the core. 0.5 M of zinc acetate dihydrate [Zn $(CH_3COO)_2 . 2H_2O$] and sodium hydroxide (NaOH) solution is used in 3% starch stock solution under constant stirring to produce ZnO nanostructures. It is observed that at first the colour of the resulting reaction solution is pale white, with further reaction time it turns milky white, confirming the formation of ZnO. A very small amount of ammonia and 0.5 M of thiourea($NH_2.CS.NH_2$)solution is used to produce the shell. The pH value of Zn complex solution was adjusted to 11. Finally, the ZnO/ZnS core/shell nanostructures are prepared with respect to change of volume ratio of core and shell matrix solution at 1:1.5(sample-I), 1:2.25 (sample –II) and 1:3 (sample-III).The formation of core-shell nanostructures was carried out by taking the as-prepared ZnO matrix solution in a cleaned glass beaker to which both Zn complex and thiourea are added alternately drop-wise, the resultant mixture being kept on constant stirring using a magnetic stirrer at high temperature for about two hrs (approx.); the appearance of dirty white colour indicates the formation of ZnO/ZnS core/shell nanocomposites. The complete synthesis method is carried out at ambient atmosphere.

All the samples thin films are grown on ordinary cleaned glass substrates for XRD studies. The samples are also arranged as colloidal solutions for optical as well as HRTEM studies. The samples films are dried in air and finally stored in airtight desiccators at room temperature for all characteristic studies.

3. CHARACTERIZATION

The as-synthesized ZnO core and their core/shell structures ZnO-ZnS are characterized via X-ray diffractometer (Seifert 3003-TT), using Cu-Kα radiation (λ= 0.15406 nm), high resolution transmission electron microscopy (HRTEM), UV-Vis, photoluminescence (PL) spectroscopy and Keithley electrometer. The XRD data are collected over an angular range of 20° < 2θ <70°with step scan 0.03000 .The morphology and structural characterizations of each samples are observed using a high resolution transmission electron microscope (JEOL JEM-2100) operating at 200 KV and the selected area electron diffraction (SAED) is also developed while HRTEM measurements are done. The optical absorption measurements were recorded using UV-visible spectrophotometer (a model-UV-1800), Shimadzu in the range 200 nm to 800nm. The photoluminescence (PL) measurements of the samples were performed using a model-F-2500 FL spectrophotometer, Hitachi with excitation wavelength of 260 nm having scan speed as 500 nm/min. The current measurements are performed with a Keithley electrometer.

4. RESULT AND DISCUSSION

Structural morphology

Fig. 1 shows the XRD pattern of the as-obtained ZnO/ZnS core/shell nanostructures. It shows the presence of diffraction peaks of both ZnO and ZnS. The spectrum of ZnO/ZnS presents a few predominant peaks centered at 31.86°, 34.44°,and 36.0°, respectively, which belong to (100), (002), and (101) diffraction planes respectively of wurtzite structured ZnO .Lattice parameters of hexagonal wurtzite ZnO are calculated from most prominent peaks using the following relation,

$$\frac{1}{d^2} = \frac{4}{3}\left[\frac{h^2 + hk + k^2}{a^2}\right] + \frac{l^2}{c^2} \qquad (1)$$

which gives lattice constant a = 3. 249 Å and c = 5.207 Å that are in well agreement with standard JCPDS data. The results are in close agreement with previous report [15]. The additional planes of ZnO are also formed at 2θ (=31.35 °, 47. 57°, 56.76° and 61.67°) which correspond to directions of the (110), (102), (110), and (103). The observed diffraction planes are in good agreement with the JCPDS file no. 36-1451.On the other hand, the diffraction peaks at 2θ (= 28.7 °, 30.51, 38.97, 48.9 and 56.73° correspond to directions of the (111), (101), (102), (220), and (311) planes of ZnS zinc blende structure and the small peak at 32.8° agrees well with the (200) plane of ZnS zinc blende structure (JCPDS 65-0309) which is being supported by earlier reports [16].

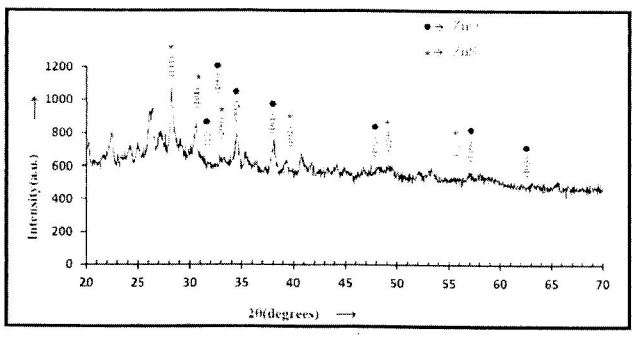

Fig. 1: XRD pattern of ZnO-ZnS core-shell nanostructure

The cubic zinc-blend structure is a steady phase at low temperatures for ZnS. The calculated lattice constant of ZnS structure is 5.406 which matches well with the values in the standard card.

The high-resolution TEM (HRTEM) measurements further support the formation of ZnO/ZnS core/shell nanostructures. The HRTEM image of as-prepared ZnO/ZnS nanostructure shows a sharp contrast between the core and the shell nanostructure [Fig.2(a)]. The SAED patterns [Fig. 2(c)] of the ZnS-ZnO core-shell shown inset of the Fig. 2 exhibit the presence of ZnO core and ZnS shell diffraction planes. It shows spotted pattern and a set of concentric ring diffraction pattern. The spots correspond to diffraction of polycrystalline ZnO and the rings are diffraction of zinc-blend structured ZnS nanoparticles. The image clearly shows the d- parameter 0.24 nm corresponding to (101) planes of ZnO and that of 0.31 nm corresponding to (002) planes of ZnS, shell[Fig.2(b)].. Similar type SAED patterns of ZnO/ZnS core /shell nanostructures have been reported by different workers [5]

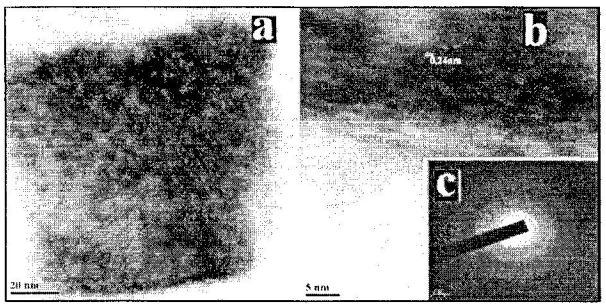

Fig. 2: (a) HRTEM image of ZnO/ZnS core-shell nanostructure, (b) d-values of ZnS and ZnO nanostructures and (c) the inset, its SAED pattern.

Optical properties

UV-visible spectroscopy

The optical absorption measurements were recorded using UV-visible spectrophotometer (a model-UV-1800), Shimadzu in the range 200 nm to 800nm. Fig. 3 shows UV-Vis spectra of ZnO-ZnS core-shell nanoparticles. The sample-I, sample-II and sample-III shows prominent excitonic absorption peaks at around 359.5 nm, 362.5 nm and 364.5 nm respectively. The excitonic absorption lies below the band gap wavelength of bulk ZnO (365 nm) [17], illustrating that the nanocomposite exhibits blue-shift compared to that of bulk ZnO, due to the quantum confinement effect. The additional small peaks may be attributed to the surface states mainly arising from dangling bonds. The band gap energy of the nanoparticles are evaluated from the UV-Vis spectra by using the formula

$$(\alpha h\nu) = c(h\nu - E_g)^{1/2} \quad (2)$$

where A is the absorption coefficient c is a constant, E_g is the band gap, and the direct band gaps estimated from a plot of $(\alpha h\nu)^2$ versus the incident photon energy $h\nu$, for sample-I, Eg=3.44eV, for sample-II, Eg=3.42eVand for sample-III, Eg=3.40 eV. Thus, with increase shell thickness, the band gap decreases, and this is agreement with PL study

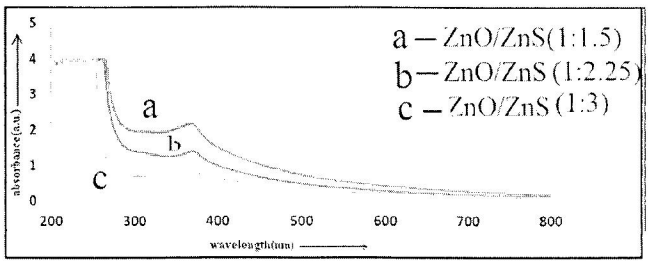

Fig. 3: Absorbance spectra of ZnO/ZnS core-shell nanostructures

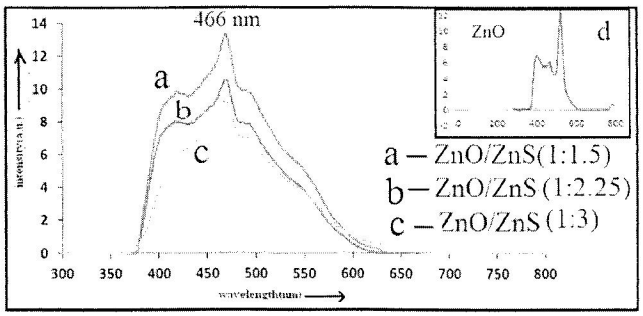

Fig. 4: PL spectra of ZnO and ZnO-ZnS core-shell nanostructures

PL spectroscopy

To investigate the optical properties as well as crystal defects of the nanostructures, photoluminescence (PL) is performed at room temperature. The photoluminescence spectra of ZnO-ZnS core-shell nanostructures (sample-I, sample - II and sample–III) embedded in starch matrix have been depicted in Fig. 4. Pl spectrum shows two excitonic peaks at 414nm and 466 nm for sample-I, 412nm and 466 nm for sample - II and 419 nm and 466 nm for sample–III and the peak at around 466nm, which is being observed in all the samples may possibly be due to band to band emission. In case of bare core ZnO, in addition to near band gap emission at 394 nm, prominent emission peak centered around 519.5 nm is also found, which mainly originates from defect states such as singly ionized oxygen vacancies; however, it is observed that the visible green emission has greatly weakened when the core is encapsulated by the shell material ZnS [Fig. 4]. It is seen that shell growth is accompanied by a red shift of the excitonic peak in the photoluminescence (PL) wavelength corresponding to bare core ZnO. This observation can be attributed to a partial leakage of the exciton into the shell material. Earlier report also evidenced the red shift of core/shell nanostructure over the core [18-20]. Moreover, there is a decrease in the emission intensity at 466 nm with increase in shell thickness that can be attributed to the increase

in non-radiative recombination. Hence, though PL intensity increases on shell coating over core; conversely, intensity found to decrease with increase in shell thickness.

Table 1: Absorption and emission characteristics of sample I sample-II and sample -III showing absorption edge (λ_a), near band gap emission (λ_e), impurity emission(λ_i) and band gap (E_g)

Sample	λ_a(nm)	λ_e(nm)	λ_i(nm)	E_g(eV)
1	359.5	414 466	486	3.44
2	362.5	412 466	487	3.42
3	364.5	419 466	486	3.40

Electrical studies

The electrical characterization is performed on the three samples by measuring the voltage with varying current at room temperature in order to see whether the film possesses ohmic or rectifying contacts [Fig. 6]. The linear nature of the characteristics *I-V* curve confirms the ohmic nature of the contact [21]. The resistances of the samples are estimated from the current-voltage data [Table-2]. An *increase of shell thickness* effects on its electrical *conductivity*. It is found that the electronic conductivity gradually increases with increase in the shell thickness. The obtained increased conductivity is the result of more spatial separation of charge carriers, the confinement of the electrons and holes in the core and shell region respectively.

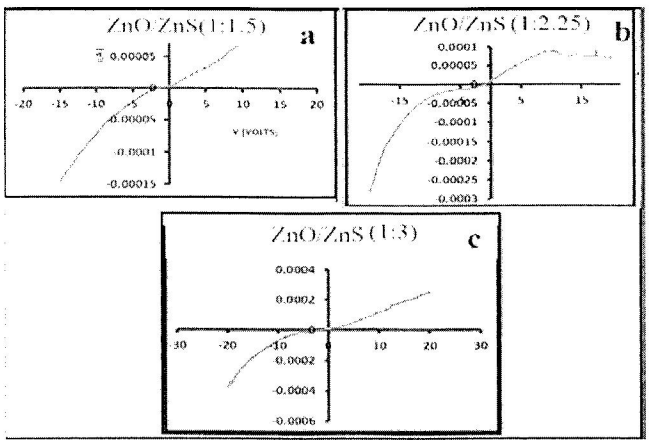

Fig. 5: Current–voltage curves of ZnO-**ZnS core-shell nanostructures**

Table 2: Core-Shell volume metric ratios and resistances of sample I sample-II and sample -III

Sample	Core/ Shell	Resistance(Ω)
1	1:1.5	154×10^3
2	1:1.25	82×10^3
3	1:1.3	106×10^3

5. CONCLUSION

In this study, we report the synthesis of ZnO-ZnS core-shell nanostructures with three different core-shell volume metric ratios (1:1.5), (1:2.25) and (1:3) via CBD method at a temperature of around 100 °C and investigate the effect of the shell thickness on the optical and photoconductive properties of the nanostructures. The results indicate that, with the increase in shell thickness, the PL intensity decreases whereas conductivity increases, which directs the separation of charge, thus ZnO-ZnS Core-Shell nanostructures may act more efficiently as photoconductors.

6. ACKNOWLEDGMENTS

Authors gratefully acknowledge Guwahati College, Guwahati for giving Laboratory facilities. We also acknowledge IITG, for XRD and I-V measurements, Department of Chemistry, Gauhati University for UV-Visible and PL measurements and SAIF, NEHU, Shillong for HRTEM measurements.

REFERENCES

[1] E. Bourgeat-Lami, "Organic-inorganic nanostructured colloids",*J. Nanosci. Nanotechnol.*, 2, 2002, pp. 1.

[2] F. Caruso, "Nanoengineering of Particle Surfaces",*Adv. Mater.*, 13, 11, 2001, pp.11–22

[3] H. Kim et al., "Characteristics of CuInS2/ZnS quantum dots and its application on LED",*J. Cryst. Growth*, 326, 2011, pp.90.

[4] M. Tomadakis, K. Mitra, "*Proc. 3-rd Inter. AIP Conf. Porous media and its applications in science, engineering and industry*", *Montecatini*, Italy, 2010, pp.181.

[5] Subhendu K. Panda, Apurba Dev, and Subhadra Chaudhuri, "Fabrication and Luminescent Properties of *c*-Axis Oriented ZnO–ZnS Core–Shell and ZnS Nanorod Arrays by Sulfidation of Aligned ZnO Nanorod Arrays",*J. Phys. Chem. C, 111*, 2007, pp. 5039-5043

[6] Kong, Y. C., Yu, D. P., Zhang, B., Fang, W., Feng, S. Q. , "Ultraviolet- emitting ZnO naosynthesized by a physical vapor deposition approach", *Appl.Phys. Lett., 78,* 2001, pp.407.

[7] Li, Y., Meng, G. W., Zhang, L. D., Phillip, F. , "Ordered Semiconductor ZnO Nanowires Arrays and Their Photoluminescence Properties," Applied Physics Letters", *Appl. Phys. Lett.*, 76, 15, 2000, pp. 2011-2013

[8] R Chakraborty, U Das, D Mohanta and A Choudhury, "Fabrication of ZnO nanorods for optoelectronic device applications.", *Indian J. Phys.*, 83, 2009, pp. 553-558.

[9] M C Newton and R Shaikhaidarov , "ZnO tetrapod p-n junction diodes", *Appl. Phys. Lett.*, **94**, 2009,pp.153112.

[10] P. Verma, A. C. Pandey, *J.* Biomater Nanobiotechnol, "Controlled Growth of CdS Nanocrystals: Core/Shell viz Matrix", 2, 2011 pp. 409-413.

[11] Samar Tarish et al. ",Synchronous Formation of ZnO/ZnS Core/Shell Nanotube Arrays with Removal of Template for Meliorating Photoelectronic Performance", *J. Phys. Chem.* , 119, C 2015, pp.1575–1582,

[12] K. Wang et al., Synthesis and photovoltaic effect of vertically aligned ZnO/ZnS core/shell nanowire arrays", *Appl. Phys. Lett.*, 96, 2010, pp.123105.

[13] M-Y. Choi, H-K. Park, M-JinJin, D. H. Yoon, S-W. Kim, "Mass production and characterization of free-standing ZnO nanotripods by thermal chemical vapor deposition" ,*J. Cryst. Growth*, 311, , 2009, pp.504-507.

[14] Sarmila Dutta, Shibabrata Basak and Pijus Kanti Samanta," Enhanced photoluminescence from ZnO/ZnS core-shell structure", *J. of Chem. Eng and Mater. Sci.* ,3,2 , March 2012 pp. 18-22.

[15] A Jegan, A Ramasubbu, K Karunakaran and S Vasanthkumar, "Synthesis and characterization of zinc oxide–agar nanocomposite", *Int. J. Nano Dimens.*, 2, 2012, pp. 171-176.

[16] Xianghua Zeng et al. "Size- and morphology-dependent optical properties of ZnS:Al one-dimensional structures",*J Nanopart Res.*, 17, 4, Apr 2015, pp.188.

[17] C Jagadish and S J Pearton , "Zinc Oxide Bulk, Thin Films and Nanostructures: Processing, Properties and Applications ", *U K: Elsevier 's Science and Technology*, 2006,pp. 6

[18] R. G. Xie, U. Kolb, J. X. Li, T. Basche, A. Mews, "Synthesis and characterization of highly luminescent CdSe-Core CdS/ZnO.5 CdO.5S/ZnS multishell nanocrystals", *J. Am. Chem. Soc.*, 127, 2005, pp. 7480-7488.

[19] A. Datta, S. K. Panda, S. Chaudhuri, "Synthesis and Optical and Electrical Properties of CdS/ZnS Core/Shell Nanorods",*J. Phys. Chem. C*, 111, 17260, 2007.

[20] Schrier J, Demchenko DO, Wang L-W., "Optical properties of ZnO/ZnS and ZnO/ZnTe heterostructures for photovoltaic applications", Nano Lett. 7,2007, pp.2377

[21] Smith R W., "Properties of ohmic contacts to cadmium sulfide single Crystals", *Phys. Rev.*, 97, 6, 1955, pp.1525.